Seismic swarm preceding the 2017 Mount Agung eruption in Bali (Indonesia) enhanced by the matched filter approach

Dimas Sianipar[1,2], Emi Ulfiana[1,3], Renhard Sipayung[1,4]

[1]Badan Meteorologi, Klimatologi, dan Geofisika (BMKG), Jakarta 10720, Indonesia

[2]Sekolah Tinggi Meteorologi, Klimatologi, dan Geofisika (STMKG), Tangerang Selatan, Banten, 15221, Indonesia

[3]BMKG Stasiun Geofisika Sanglah, Denpasar, Bali, Indonesia

[4]BMKG Stasiun Geofisika Banjarnegara, Jawa Tengah, Indonesia

Corresponding author: Dimas Sianipar (https://orcid.org/0000-0002-9895-4616)

Email: dsj.sianipar@stmkg.ac.id, dimas.salomo@bmkg.go.id

Key Points:

- Reappraisal of the seismic swarm preceding the 2017 Mount Agung eruption by waveform-based relocation and matched filter technique.
- We detect fourteen times more events (5,803 earthquakes) than the routine earthquake catalog (407 earthquakes).
- We show the updated spatiotemporal evolution of the swarm seismicity before the eruption.

Abstract

Intense swarm seismicity took place before the 2017 Mount Agung eruption in Bali (Indonesia). However, the earthquake sequences were not well documented. In addition, there was a substantial delay between the peak of the seismic activity (late September) and the onset of the impending eruption (late November). We applied waveform-based hypocenter relocation and matched filter technique (MFT) to enhance the earthquake catalog of the swarm associated with the eruption. We detect fourteen times more events (5,803) than the routine catalog (407) from 1 August 2017 to 1 December 2017. The intense swarm initiated on 20 September 2017 at ~09:00 UTC, and the peak of the swarm occurred during 22-24 September with 1,473 events. The updated spatiotemporal evolution of the swarm seismicity shed light on the processes involved in a volcano reawaking and highlighted the use of MFT in volcano monitoring with existing regional seismic networks.

Plain Language Summary

The sequence of earthquake swarms before the Mount Agung eruption in 2017 was not well investigated due to the lack of local seismic observations close to the summit. We overcome this limitation by applying advanced seismic relocation and detection using an existing regional seismic network routinely used for ‘tectonic’ earthquake monitoring in Indonesia. The detection approach benefits from waveform cross-correlations between the digital-continuous seismograms and template seismograms. We detect and locate fourteen times more earthquakes than that of had been cataloged by regular earthquake monitoring in Bali, Indonesia. The more robust and improved swarm catalog provides information about processes during the volcanic unrest of Mount Agung before the impending eruptions.

Index Terms:

Volcano Seismology

Volcano Monitoring

Earthquake Source Observations

Seismic Instruments and Networks

Keywords: Mount Agung, Matched Filter, Earthquake Swarm, Volcano-Tectonic (VT)

1. Introduction

Mount Agung is a ~3000-m high stratovolcano that dominates the northeastern zone of Bali Island in Indonesia (Figure 1). After having been inactive since 1963-64, Mount Agung erupted for the first time in late November 2017. Previous studies indicated a frequency of one explosive eruption (VEI≥2-3) per century (on average) for Mount Agung, and in its ~5000-year record, marked by periods of background-eruptive rates identical to general subduction zone volcanoes then changed to durations of increased eruptive rates (Fontijn *et al.*, 2015). This dynamic has been attributed to increased magma supply rates from a depth suggesting various open-system processes of magmatic differentiation. Its magmas formed by repeated intrusions of basaltic magmas into basaltic andesitic to andesitic reservoirs (Fontijn *et al.*, 2015). It is noteworthy that the 1963-64 Mount Agung eruption yielded serious fatalities with almost 1,500 people killed by its pyroclastic flows and fast-flowing volcanic mudflows (lahars).

The timeline during the 2017 volcanic crisis of Mount Agung has been described in previous studies (e.g., Albino *et al.*, 2019; Syahbana *et al.*, 2019). The first phreatomagmatic eruption occurred on 21 November, and the onset of the magmatic eruption occurred on 25 November (Syahbana *et al.*, 2019). These eruptions were preceded by a series of energetic seismic swarms (Figure 1). However, these earthquakes were not well cataloged. It remains unclear about the source origin of this swarm and its spatiotemporal evolution as well as its association with the eruption. The lack of information about this swarm is due to the lack of capability in detecting small earthquakes by the routine methodology applied in regular monitoring. Moreover, the 2017 seismic swarm occurred without immediate eruption; the eruption began about several weeks after the seismicity had already decreased. Robust information about precursory seismic swarm during a volcanic crisis is important for proper response and eruption forecasting.

In this study, we perform a matched filter technique (MFT; or template matching) to identify small, uncatalogued earthquakes based on their similarity to target events (i.e., templates). Zhang and Wen (2015) and Kato *et al.* (2015) also utilized a similar technique to swarm seismicity preceding eruptions of Mount Ontake in Japan. We provide a more complete and improved catalog of the swarm seismicity and then summarize the 2017 unrest at Mount Agung by showing the swarm's updated spatiotemporal evolution based on the MFT catalog. We highlight the application of MFT in monitoring volcanic swarm using the existing regional broadband seismic network.

2. Data and Methods

Based on the national catalog of Badan Meteorologi, Klimatologi, dan Geofisika (BMKG), the seismicity near Mount Agung from September to November 2017 located mostly NW of Mount Agung (Figure S1, S2). Some 407 events had been identified by BMKG with magnitudes ranging from 2.2 to 4.9 and depths between 5 and 20 km (Figure 1a, b). The magnitude of completeness (*Mc*) of this catalog is 2.7 (local magnitude, Figure S3). The seismicity contains many smaller earthquakes than larger events, yielding a relatively large b-value of frequency-magnitude distribution (FMD), i.e., b= 1.3 (Figure 1d, S3).

All of the earthquakes considered here are the type of volcano-tectonic (VT) earthquakes shown by their high-frequency contents (Figure S4-S7), clear P- and S-wave arrivals on their seismograms (Figure 2), and locations adjacent to the volcanoes (Chouet and Matoza, 2013; Roman and Cashman, 2006; McNutt, 2005; Lahr *et al.*, 1994). However, we observe obvious S-wave shadow at station SRBI and DNP (Figure 2, S8), and we will discuss this topic in the discussion section. We pick P- and S-wave arrival times for the 407 events and enhance the quality of locations by applying double-difference relocation improved with waveform cross-correlation data (Waldhauser and Ellsworth, 2000, see Text S1, Figure 3).

In this study, we use all of these 407 events as template candidates for MFT. MFT employs many template waveforms and identifies small events through multi-station waveform cross-correlation (Meng *et al.*, 2018). The MFT has also been applied in other volcanic areas, such as at Piton De La Fournaise volcano (Duputel *et al.*, 2019).

We collected the waveform data for all of these earthquakes and used them as templates candidates in scanning through the continuous waveforms for earthquakes associated with the 2017 eruption. We selected data from six regional broadband three-component stations (i.e., 18 channels) with a distance less than 170 km from the summit and with good azimuthal coverage to investigate the swarm associated with the eruption (Figure 1, 4).

The MFT procedure here generally follows that of Meng *et al.* (2013; 2018). We use continuous waveforms containing each 24-hours seismogram for a period of 1 August to 1 December 2017 (i.e., 123 days). We use SH* channels data with a sampling rate of 40 Hz. A two-way pass, fourth-order, Butterworth band-pass filter with a corner frequency of 1 and 15 Hz was applied to both continuous and template waveforms. Among 407 template candidates, we select quality seismograms of 257 templates that have been satisfactorily relocated and having signal-to-noise ratio (SNR) >5 recorded by at least eight channels (≥ 3 stations).

The template waveform comprises signals within a time window of 8 s starting from 0.5 s before the picked P-wave arrival time for the vertical component and 0.5 s before the picked S-wave arrival time for the two horizontal components. We compute the correlation-coefficient (CC) between the template and continuous waveform by using a correlating time step of 0.025 s; i.e., the computing window moves forward by one data point.

We compute the mean CC among all components at each time point, allowing one data point shift (Meng *et al.*, 2013). A perfect self-detection should have a mean CC of 1, i.e., the template waveforms should perfectly detect itself in the continuous waveforms. To ensure the quality of detection, we use a high threshold (Meng *et al.*, 2013). The newly positive detection threshold is the sum of the median value and 15 times the median absolute deviation (MAD) of the mean CC trace. Using a lower threshold (e.g., 6-14 x MAD as applied in some references) would result in false detections.

The detected event location is assigned to be the same as that of the corresponding template with the highest mean CC within 2 s, assuming that the template and new detected event are collocated based on their high correlation. The detected event magnitude is computed based on the peak amplitude ratios between the detected and template event (Meng *et al.*, 2013). An example of MFT detection is provided in Figure 4 and S9.

3. Results

Waveform-based hypocenter relocation indicates most of the events located between Mount Agung and Batur Caldera, but closer to Mount Abang (Figure 2). There is also one obvious separated cluster in the NE of Mount Agung (Figure 3). The relocation indicates all events took place at depths 6.8 to 13.1 km (mostly at 9 to 13 km) or in the mid-crust (Figure 3, S12). It is noteworthy that Geiger *et al.* (2018) proposed two major magma storage regions of Mount Agung located at 18 to 22 km depth (near the Moho discontinuity) and 3 to 7 km depth. In other words, the seismicity located midway between the deeper and shallower magma storage zone.

Using a relatively high threshold, we detect 5,803 events, including 257 perfect self detections with mean CC= 1 (Figure 5). This number is equivalent to about fourteen times the number of events reported by BMKG. Completeness of the MFT catalog is 2.4 (local magnitude), lower than 2.7 of the BMKG catalog (Figure S3). The magnitudes range from 1.5 to 4.9, and 20 events have magnitude >3.5 (Figure 5d); one of them is newly detected, i.e., the 2017-10-18 00:24 UTC with magnitude 3.6. As expected, because MFT detects small magnitudes, the b-value for the entire seismicity increases became b= 1.6.

Some new detections have a large correlation with the detecting templates; for example, a magnitude 3.1 (Figure S9, Table S2) is newly detected with mean CC of 0.946 on 21 September 09:07:17 UTC by template 20170921104359 (M=3.3; 12 channels with SNR > 5). Another example is a magnitude 3.1 on 13 October 15:32 UTC detected with mean CC of 0.857 by a magnitude 3.6 template (Figure 4).

We detect only two small events that occurred in the first 50 days (from 1 August to 19 September) with magnitude 2.7 and 2.6 (15 August), respectively (Figure S10, S11). Intense seismicity initiated on 20 September at 09:00 UTC with a small event at depth ~9.7

km and located closer to Mount Agung (Figure 5). We detect 85 events during the day of 20 September as compared to only two events in the BMKG catalog. The seismicity rapidly accelerated, and more than 300 events per day were detected during 21-26 September, while the peak of the swarm occurred from 22 to 24 September (UTC) with 1,473 detected events (indicated by the first green line on Figure 5a).

The seismicity during 20-22 September mostly occurred at ~9 to 11 km depths, however, during the early peak period with the rapid acceleration of seismicity (started on 22 September), the earthquakes were located at deeper locations up to ~13 km in the mid-crust (Figure 5b). The rate of seismicity also slightly increase on 26 and 27 September due to the existence of two M>4 events (black stars in Figure 5a). We observe three obvious peaks in the number of earthquakes on 23 September, 6 October, and 18 October 2017 (Figure 5a). The increase of seismicity in mid-October 2017 was also accompanied by some deeper events. Seismicity decreased on 20-21 October (< 20 events per day, marked by the second green line on Figure 5a).

The total duration of the intensive swarm (e.g., with > 6 detected events per day) was 39 days, i.e., 20 September to 28 October. After about ten days of quiescence (e.g., ≤ six events per day), the seismicity rate increased slightly on 8 November due to an M4.9 earthquake (marked by the third green line on Figure 5a) and its early aftershocks. However, these earthquakes appeared in a different location, NE of Mount Agung.

4. Discussions and Conclusion

In this study, we perform hypocenter relocation and MFT to enhance the detection of lower magnitude VT events before the 2017 Mount Agung eruption. We decreased the completeness of the swarm catalog from 2.7 to 2.4, and the FMD is better fitted as cumulative normal distribution than that of the BMKG catalog (Figure S3). Mount Agung has swarm seismicity with the maximum peak in the opening of the sequence. Seismicity continued to accelerate rapidly toward its peak in just one day after the detectable initiation.

Hypocenters of the swarm can also be divided into two groups. The first group is the denser seismicity beneath Mount Agung and Batur Caldera (Figure 3d). Most of the refined seismicity during the peak of the swarm located in this group and persistently took place at ~9-11 km depth with only two occurrences at the deeper location (up to 13 km depth), i.e., when the peak seismicity occurred (22 September) and on mid-October. The episode of earthquakes at deeper locations in a short period during 22 September is interesting. This episode might pronounce the initiation of a dike intrusion. VT seismicity was considered to reflect the stresses induced by the dike propagation (e.g., Roman and Cashman, 2006).

Another group is a sequence that contains the 8 November M4.9 and its aftershocks located ~8-10 km NE of Mount Agung. Their epicenters formed a NE-SW lineament (Figure 2), and the hypocenters probably formed a dipping structure (Figure 3). We interpret this cluster as seismicity occurred at a local tectonic fault. The seismicity in this cluster was recorded in a station DNP (SW of epicenters) with no obvious S-wave (or so-called 'S-wave shadow', Figure S8) because the propagation of seismic rays might go through the magma plumbing zone of Mount Agung. This observation also marks a potentially seismic detection of a magma reservoir beneath Mount Agung by S-wave shadow (e.g., Lin *et al.*, 2018; Harjono *et al.*, 1989). In contrast, the S-wave of the M4.2 event (26 September) from the first cluster is clear at station DNP but hardly observed at station SRBI (NW of the epicenter), as shown in Figure 2. This S-wave shadow might be due to the existence of magma beneath either Mount Abang and Batur Caldera.

After the M4.9 event, Pusat Vulkanologi dan Mitigasi Bencana Geologi (PVMBG) of Indonesia reported the emergence of low-frequency (LF) events and volcanic tremors beneath Mount Agung (Figure 5). However, the proximal shallow seismic activity associated with the impending eruption might be small-magnitudes (e.g., M<2.4). Thus, the regional network could not detect these events through our MFT detection, and its progression toward the summit might only be detected by very close seismic stations.

Syahbana *et al.* (2019) reported that the intense swarm had been initiated on 16 September, as shown by the increase of Real-time Seismic Amplitude Measurement (RSAM) at a local short-period station (Figure 5c). However, in this study, MFT detection by using a regional network indicates that the swarm was initiated on 20 September ~09:00 UTC. This discrepancy might indicate that the seismic events from 16 to 19 September were smaller than 2.4, above which our MFT catalog can be considered complete by the regional station's observation. In general, the pattern of seismicity rate changes determined by MFT detection (Figure 5a) is similar to the RSAM graph from the local short-period station (Figure 5c). The swarm accelerated on 22 September 2017, as shown by the seismic record at a local station (RSAM values peaked on 22 September in station TMKS).

Syahbana *et al.* (2019) inferred that magma intruded into the mid-crust in early 2017 and in August 2017, in advance of the intrusion of a dike between Mount Agung and Abang that initiated swarm seismicity in late September. The record of the N component of REND (GNSS) indicated ~20 cm southward movement (Figure 5c) from August to late September, away from Mount Agung. Syahbana *et al.* (2019) interpreted this displacement as a sign of deep inflation beneath Mount Agung. This deep inflation was aseismic, confirmed by the RSAM of TMKS station and the MFT detection in this study (Figure 5). The intense swarm activity was initiated near the end of this deep inflation. During the period of 16 to 23 September, the REND displacement was changing become northward movement. Syahbana *et al.* (2019) interpreted this northward movement (toward Mount Agung) as the sign of deep deflation.

Using InSAR analysis and 3D numerical models, Albino *et al.* (2019) indicated the 2017 seismic swarm was related to the intrusion of a deep, sub-vertical magmatic dike between Agung and Batur. Their inferred dike is plotted in Figure 3. Our swarm seismicity in this study is generally consistent with the location of the dike proposed by them (Figure 3). We agree about a vertically and laterally interconnected system undergoing recurring magma mixing beneath Mount Agung and Batur. Based on Albino *et al.* (2019), a scheme of transport from a deep mafic source to a shallow andesitic reservoir is consistent with the 2017 dike's geometry, while stresses from the topographic load controlled it. Besides, the corrected InSAR time series indicates a broad pre-eruptive uplift (Figure 5b) between Mount Agung and Batur (Point 'A', Figure 2) primarily during 6 to 14 October or about two weeks after the initiation of the swarm and one month before the eruption (Albino *et al.*, 2020). This uplift corresponds to the general decreases in VT earthquakes' rate with one of the little peaks of the seismicity shown in Figure 5.

Volcanic unrest and eruption at Agung provide important lessons for eruption forecasting (Gertisser *et al.*, 2018). The uncertainties in forecasting the eruption at Agung was due to the local seismic data limitations. Here, we attempted to overcome the limitation of small earthquake detection using an existing regional network. The intensive period of the Agung's VT swarm occurred from 20 September to 28 October (39 days), while the peak of seismicity occurred from 22 to 24 September (UTC). We identify two clusters of seismicity, i.e., in NW of Mount Agung (i.e., magmatic dike) and NE of Mount Agung (i.e., tectonic fault structure). However, we also could not detect the proximal shallow seismicity that occurred just before the eruption. Moreover, the updated spatiotemporal evolution and cumulative seismic moment of VT events (Figure S12) provided by MFT detection could help estimate the ongoing situation beneath Mount Agung.

The potential trigger mechanism for a 'late' eruption at a stratovolcano is essentially challenging to assess; in this case, it might be the deep intrusion of magma, dike-induced swarm, or the tectonic triggering from the M4.9 event. Because seismicity initially declined after the 39-days dike-induced swarm and the low-frequency (LF) and volcanic tremor events shortly took place after the M4.9 (Syahbana *et al.*, 2019), we tend to select the mechanism of that M4.9 could catalyze the eruption by either the permanent displacement (static triggering) or propagation of seismic waves (dynamic triggering) (e.g., McNutt, 2005; Walter *et al.*, 2007). Understanding every signal that came from beneath Mount Agung is important for volcanic hazard for the people of Bali and beyond. Our results show improvements in the earthquake catalog of the seismic swarm that feasibly applied shortly for monitoring of Mount Agung using existing regional networks.

Acknowledgments

Earthquake catalog can be downloaded from the BMKG repository (http://repogempa.bmkg.go.id/repo_new/repository.php) and is available in Table S1 and S2. Dataset for hypocenter relocation and MFT used in this study can be accessed from Zenodo (https://doi.org/10.5281/zenodo.3820934). All figures are created by using Generic Mapping Tools (GMT) (Wessel *et al.*, 2013). We are thankful to Xiaofeng Meng and Zhigang Peng for the matched filter code. We also thank PVMBG of Indonesia for continuous efforts in the monitoring of Mount Agung. The manuscript benefits from earthquakes information by Daryono (BMKG). Constructive comments from Fabien Albino to the early draft of this manuscript are greatly appreciated. We thank two anonymous reviewers for their comments and suggestions to the early version of this manuscript.

References

Albino, F., J. Biggs, C. Yu, and Z. Li (2020), Automated methods for detecting volcanic deformation using Sentinel-1 InSAR time series illustrated by the 2017–2018 unrest at Agung, Indonesia, *Journal of Geophysical Research: Solid Earth*, 125, e2019JB017908. https://doi.org/10.1029/2019JB017908

Albino, F., J. Biggs, and D.K. Syahbana (2019), Dyke intrusion between neighbouring arc volcanoes responsible for 2017 pre-eruptive seismic swarm at Agung, *Nat Commun*, 10(1), 748. https://doi.org/10.1038/s41467-019-08564-9.

Chouet, B. A., and R. S. Matoza (2013), A multi-decadal view of seismic methods for detecting precursors of magma movement and eruption, *Journal of Volcanology and Geothermal Research*, 252, pp.108-175.

Duputel, Z., O. Lengliné, and V. Ferrazzini (2019), Constraining Spatiotemporal Characteristics of Magma Migration at Piton De La Fournaise Volcano From Pre-eruptive Seismicity, *Geophysical Research Letters*, 46(1), pp.119-127.

Fontijn, K., F. Costa, I. Sutawidjaja, C.G. Newhall, and J.S. Herrin (2015), A 5000-year record of multiple highly explosive mafic eruptions from Gunung Agung (Bali, Indonesia): implications for eruption frequency and volcanic hazards, *Bulletin of Volcanology*, 77(7), p.59.

Geiger, H., V.R. Troll, E.M. Jolis, F.M. Deegan, C. Harris, D.R. Hilton, and C. Freda (2018), Multi-level magma plumbing at Agung and Batur volcanoes increases risk of hazardous eruptions, *Scientific Reports*, 8(1), pp.1-14.

Gertisser, R., F.M. Deegan, V.R. Troll, and K. Preece (2018), When the gods are angry: volcanic crisis and eruption at Bali's great volcano, *Geology Today*, 34(2), pp.62-65.

Harjono, H., M. Diament, L. Nouaili, and J. Dubois (1989), Detection of magma bodies beneath Krakatau volcano (Indonesia) from anomalous shear waves, *Journal of Volcanology and Geothermal Research*, 39(4), pp.335-348.

Kato, A., T. Terakawa, Y. Yamanaka, Y. Maeda, S. Horikawa, K. Matsuhiro, and T. Okuda (2015), Preparatory and precursory processes leading up to the 2014 phreatic eruption of Mount Ontake, Japan, *Earth, Planets and Space*, 67(1), pp.1-11.

Lahr, J. C., B. A. Chouet, C. D. Stephens, J. A. Power, and R. A. Page (1994), Earthquake classification, location, and error analysis in a volcanic environment: Implications for the magmatic system of the 1989–1990 eruptions at Redoubt Volcano, Alaska, *Journal of Volcanology and Geothermal Research*, 62(1-4), pp.137-151.

Lin, C.H., Y.C. Lai, M.H. Shih, H.C. Pu, and S.J. Lee (2018), Seismic Detection of a Magma Reservoir beneath Turtle Island of Taiwan by S-Wave Shadows and Reflections, *Scientific Reports*, 8(1), pp.1-12.

McNutt, S.R. (2005), Volcanic seismology, *Annu. Rev. Earth Planet. Sci.*, 32, pp.461-491.

Meng, X., H. Yang, and Z. Peng (2018), Foreshocks, b value map, and aftershock triggering for the 2011 Mw 5.7 Virginia Earthquake, *Journal of Geophysical Research: Solid Earth*, 123(6), pp.5082-5098.

Meng, X., Z. Peng, and J.L. Hardebeck (2013), Seismicity around Parkfield correlates with static shear stress changes following the 2003 Mw6.5 San Simeon earthquake, *Journal of Geophysical Research: Solid Earth*, 118(7), pp.3576-3591.

Roman, D.C. and K.V. Cashman (2006), The origin of volcano-tectonic earthquake swarms, *Geology*, 34(6), pp.457-460.

Syahbana, D.K., K. Kasbani, G. Suantika, O. Prambada, A.S. Andreas, U.B. Saing, S.L. Kunrat, S. Andreastuti, M. Martanto, E. Kriswati, and Y. Suparman (2019), The 2017–19 activity at Mount Agung in Bali (Indonesia): Intense unrest, monitoring, crisis response, evacuation, and eruption, *Scientific Reports*, 9(1), pp.1-17.

Waldhauser, F. and W.L. Ellsworth (2000), A double-difference earthquake location algorithm: Method and application to the northern Hayward fault, California, *Bulletin of the Seismological Society of America*, 90(6), pp.1353-1368.

Walter, T.R., R. Wang, M. Zimmer, H. Grosser, B. Lühr, and A. Ratdomopurbo (2007), Volcanic activity influenced by tectonic earthquakes: static and dynamic stress triggering at Mt. Merapi, *Geophysical Research Letters*, 34(5).

Wessel, P., W.H. Smith, R. Scharroo, J. Luis, and F. Wobbe (2013), Generic mapping tools: improved version released, *Eos, Transactions American Geophysical Union*, 94(45), pp.409-410.

Wiemer, S. (2001), A software package to analyze seismicity: ZMAP, *Seismological Research Letters*, 72(3), pp.373-382.

Zhang, M. and L. Wen, (2015), Earthquake characteristics before eruptions of Japan's Ontake volcano in 2007 and 2014, *Geophysical Research Letters*, 42(17), pp.6982-6988.

Figure 1. VT swarm before the 2017 Mount Agung eruption. **(a)** Spatial distribution of epicenters (colored circles) from 1 August to 1 December 2017. Circles are scaled to magnitude. Inverted triangles are BMKG broadband seismic stations. **(b)** Magnitude distribution. Blue solid lines are the cumulative number of earthquakes. **(c)** Spatiotemporal N-S distribution. **(d)** Histogram of frequency-magnitude distribution.

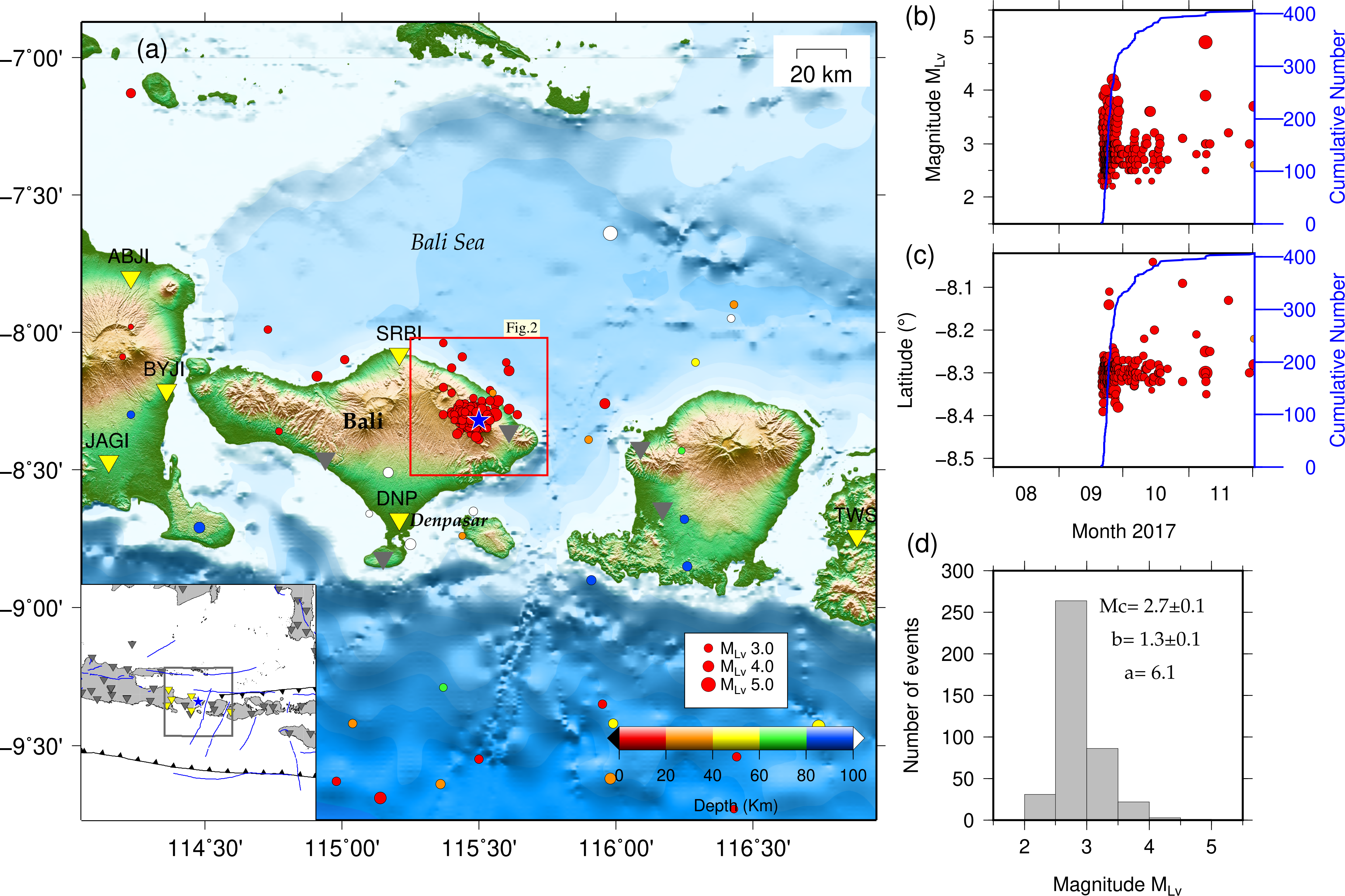
(a)
20 km
Bali Sea
ABJI
SRBI
BYJI
JAGI
DNP
TWS
Fig.2
Bali
Denpasar
M Lv 3.0
M Lv 4.0
M Lv 5.0
Depth (Km)
0 20 40 60 80 100
-7°00'
-7°30'
-8°00'
-8°30'
-9°00'
-9°30'
114°30'
115°00'
115°30'
116°00'
116°30'
(b)
Magnitude M Lv
Cumulative Number
(c)
Latitude (°)
Month 2017
08 09 10 11
(d)
Number of events
Magnitude M Lv
Mc= 2.7±0.1
b= 1.3±0.1
a= 6.1

Figure 2. The topography around Mount Agung and relocated epicenters of VT swarm (red circles). Squares are TMKS, PSAG (seismic), and REND (GNSS) station. Stars are M>4 events. Also shown three-component seismograms of station SRBI and DNP for the 26 September 2017 M4.2 event.

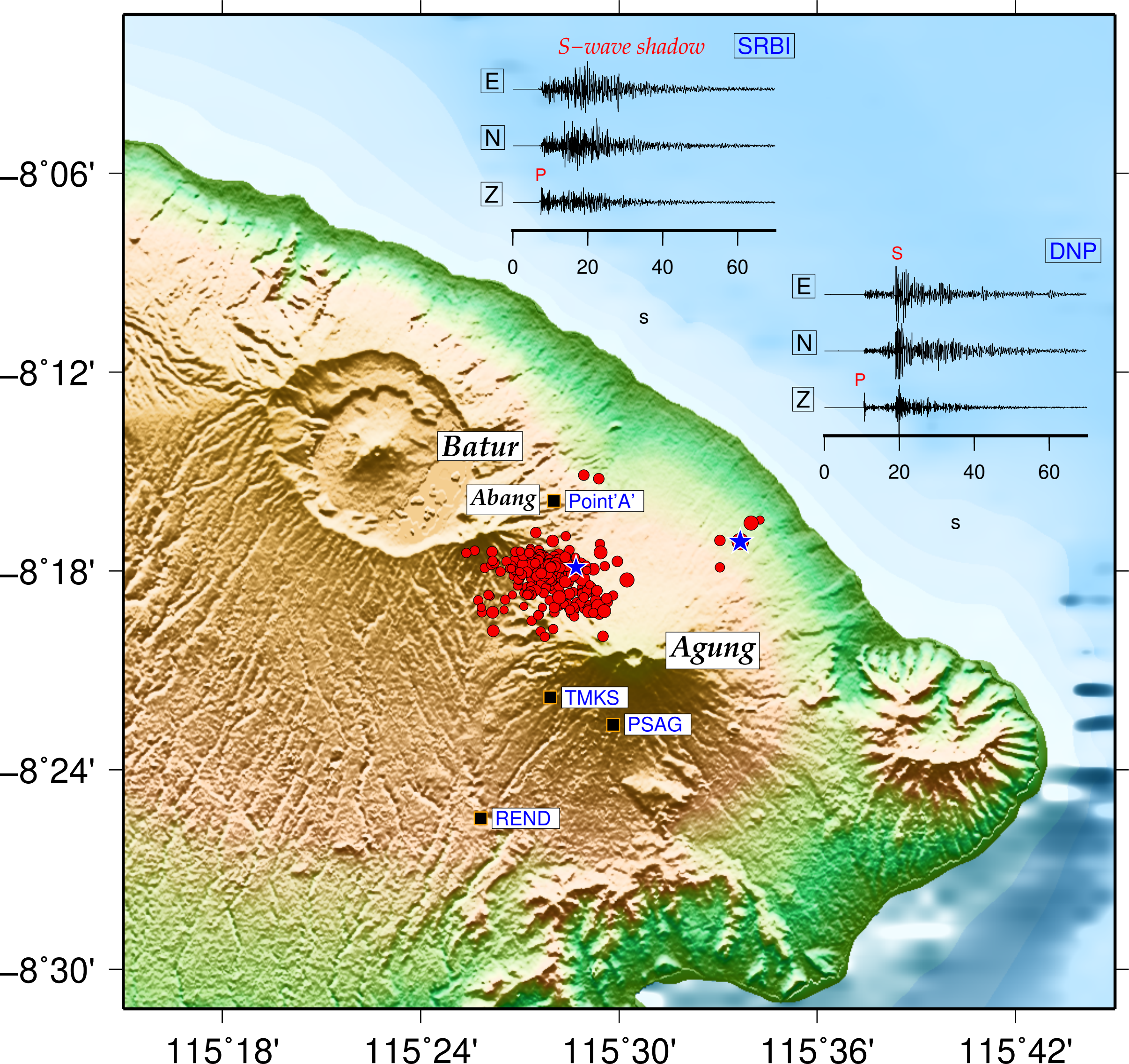

S−wave shadow
SRBI
E
N
Z
P
0
20
40
60
s
DNP
S
E
N
P
Z
0
20
40
60
s
Batur
Abang
Point'A'
Agung
TMKS
PSAG
REND
−8°06'
−8°12'
−8°18'
−8°24'
−8°30'
115°18'
115°24'
115°30'
115°36'
115°42'

Figure 3. Relocated hypocenters. **(a)** Along the S-N profile. **(b)** Along the SW-NE profile. **(c)** Along the W-E profile. **(d)** Along the NW-SE profile. Orange solid rectangles represent dike inferred by Albino *et al.* (2019).

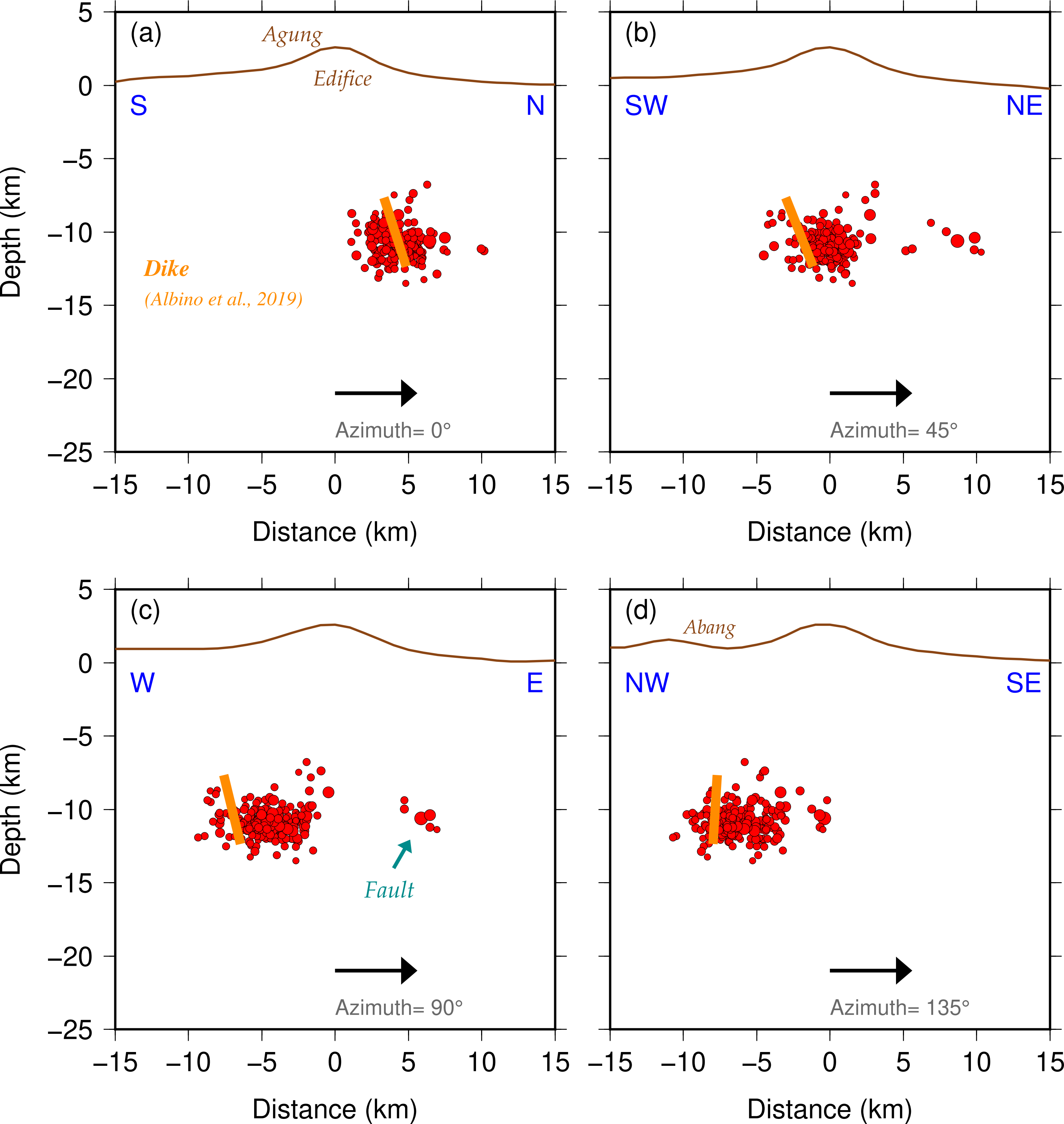

(a)
Agung
Edifice
S
N
Dike
(Albino et al., 2019)
Azimuth= 0°
(b)
SW
NE
Azimuth= 45°
(c)
W
E
Fault
Azimuth= 90°
(d)
Abang
NW
SE
Azimuth= 135°
Depth (km)
Distance (km)

Figure 4. MFT detection. Example of waveform comparison between a detected event (magnitude 3.1; gray traces) and its detecting template event (magnitude 3.6; red traces). The mean correlation coefficient between all of these waveforms is 0.857. The black arrow shows the origin time of the detected event. The amplitudes were normalized by the maximum value at each window at each component/station. The station name, component/channel, and distance (km) are shown at the beginning of each gray trace. Station locations are plotted in the inset figure.

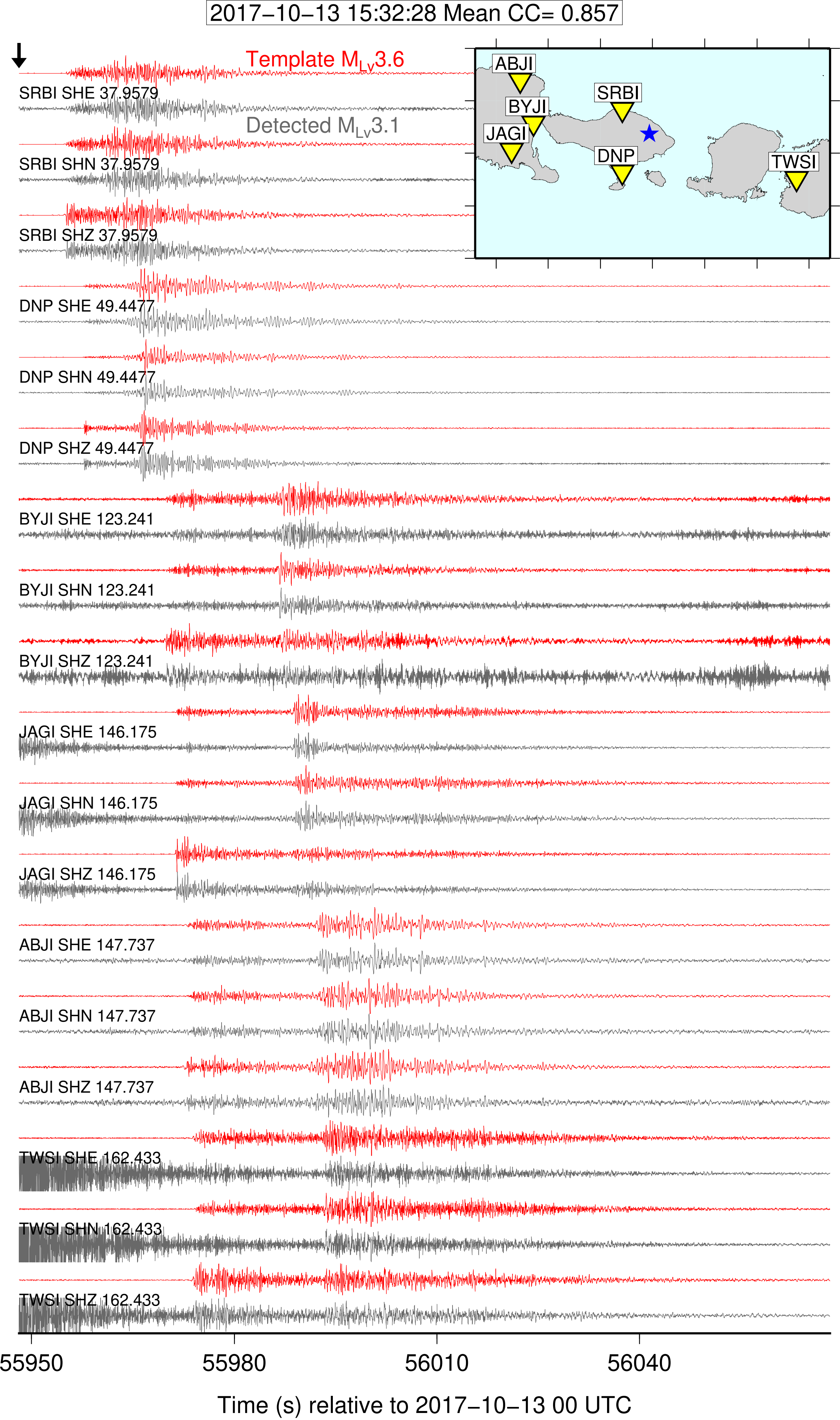
2017−10−13 15:32:28 Mean CC= 0.857
Template M_{Lv}3.6
Detected M_{Lv}3.1
ABJI
BYJI
JAGI
SRBI
DNP
TWSI
SRBI SHE 37.9579
SRBI SHN 37.9579
SRBI SHZ 37.9579
DNP SHE 49.4477
DNP SHN 49.4477
DNP SHZ 49.4477
BYJI SHE 123.241
BYJI SHN 123.241
BYJI SHZ 123.241
JAGI SHE 146.175
JAGI SHN 146.175
JAGI SHZ 146.175
ABJI SHE 147.737
ABJI SHN 147.737
ABJI SHZ 147.737
TWSI SHE 162.433
TWSI SHN 162.433
TWSI SHZ 162.433
55950
55980
56010
56040
Time (s) relative to 2017−10−13 00 UTC

Figure 5. Swarm seismicity detected by MFT. **(a)** Spatiotemporal evolution of VT earthquakes (circles; colored according to the depth of the hypocenters). Gray triangles are templates. Black stars are M>4.1 events. L2, L3, and L4 correspond to the different alert levels provided by the PVMBG during the crisis. LF=Low Frequency events. The first and second green lines denote the time mark of 22 September and 20 October, respectively (see text). The third green line denoted the time mark when a magnitude 4.9 occurred. The blue dashed line indicates a time mark when the tremor firstly took place. The first and second red lines indicate when the first phreatomagmatic eruption and the onset of larger explosions, respectively. Blue solid line shows the number of earthquakes per day based on MFT detection. **(b)** Depth-time evolution of VT earthquakes. Solid lines show the corrected InSAR time series detecting displacement anomalies at point 'A' (see Fig. 2) provided by Albino *et al.* (2020). **(c)** GNSS time-series from station REND (N) and 12 hours RSAM from station TMKS (Syahbana *et al.*, 2019). **(d)** Magnitude distribution of MFT-based VT seismicity colored by different detection thresholds. Red circles are templates. The solid blue line corresponds to the cumulative number of events.

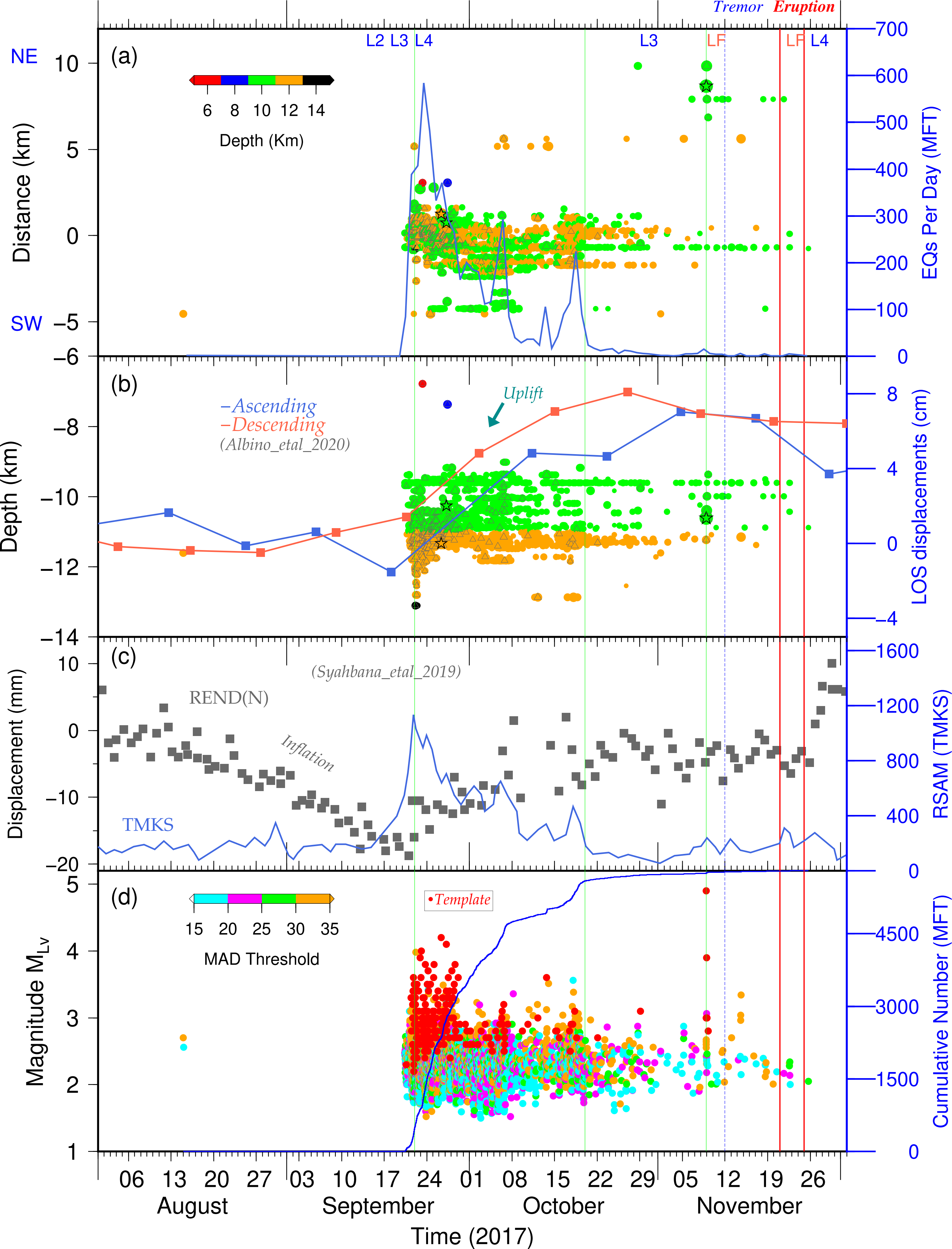

Tremor
Eruption
(a)
L2 L3 L4
L3
LF
LF L4
NE
SW
Distance (km)
EQs Per Day (MFT)
6 8 10 12 14
Depth (Km)
(b)
Depth (km)
LOS displacements (cm)
–Ascending
–Descending
(Albino_etal_2020)
Uplift
(c)
Displacement (mm)
RSAM (TMKS)
(Syahbana_etal_2019)
REND(N)
Inflation
TMKS
(d)
Magnitude M_{Lv}
Cumulative Number (MFT)
•Template
15 20 25 30 35
MAD Threshold
06 13 20 27 03 10 17 24 01 08 15 22 29 05 12 19 26
August
September
October
November
Time (2017)

Supporting Information for

Seismic swarm preceding the 2017 Mount Agung eruption in Bali (Indonesia) enhanced by the matched filter approach

Dimas Sianipar[1,2], Emi Ulfiana[1,3], Renhard Sipayung[1,4]

[1]Badan Meteorologi, Klimatologi, dan Geofisika (BMKG), Jakarta 10720, Indonesia

[2]Sekolah Tinggi Meteorologi, Klimatologi, dan Geofisika (STMKG), Tangerang Selatan, Banten, 15221, Indonesia

[3]BMKG Stasiun Geofisika Sanglah, Denpasar, Bali, Indonesia

[4]BMKG Stasiun Geofisika Banjarnegara, Jawa Tengah, Indonesia

Contents of this file

Additional Supporting Information (Files uploaded separately)

Captions for Figure S1 to S12

Captions for Table S1 to S2

Text S1. [Hypocenter Relocation]

We selected seismic data from six BMKG regional broadband three-component stations (i.e., 18 channels) with a distance less than 170 km from the summit and with good azimuthal coverage, i.e., station SRBI (~37 km), DNP (~49 km), BYJI (~123 km), JAGI (~146 km), ABJI (~147 km), and TWSI (~162 km). We lacked a local broadband station close to the summit of Mount Agung (Fig. 2, S8); however, two of our stations located within <50 km distance from Mount Agung. It is noteworthy that Pusat Vulkanologi dan Mitigasi Bencana Geologi (PVMBG) operated two short-period seismic stations during the 2017 unrest located on the S and SW flanks of Mount Agung, ~4 and 5 km from the summit, i.e., station TMKS and PSAG (Fig. 2). Besides, station REND is one of five continuous GNSS stations that used to monitor the deformation of Mount Agung. This station located ~12 km S-SW of the volcano's summit (Fig. 2).

We visually picked the arrival times of the P- and S-waves of 407 VT earthquakes between 1 August and 1 December 2017. In addition to the catalog of arrival times, we also used differential arrival times obtained by the waveform cross-correlation method. The time window for cross-correlation is within a 2s; 0.5 s before and 1.5 s after the hand-picked P/S arrival times for seismograms bandpass filtered between 1 and 15 Hz. We relocated the events using double-difference method applied in HypoDD code (Waldhauser and Ellsworth, 2000). We used the global 1D velocity model (IASP91; Kennett and Engdahl, 1991) because the local velocity structure of Mount Agung has not been previously investigated. We also attempt to use the generic volcano velocity model of Lesage *et al.* (2018) interpolated with the Crust 1.0 model (Laske *et al.*, 2013) for the region around Mount Agung. The maximum hypocentral separation is 5 km, and the maximum number of neighbors per event is 20. The minimum four links are chosen for clustering. Fig. S1 and S2 show the position of earthquakes before relocation, and Fig. 1 and 2 show the refined positions after the relocation. The relocated hypocenters mostly located at 9 to 13 km of depths (Fig. 3).

Text S2. [Magnitude Homogenization]

All of the preferred magnitude used in the BMKG catalog for earthquakes analyzed in this study was in the type of M_{LV} (local magnitude measured on the vertical component), except for the 8 November 2017 21:54 UTC event used moment magnitude (Mw=4.9). The local magnitude (M_{LV}) for this event is 5.2.

Text S3. [Calculation of Mc and b-value]

We calculated the magnitude of completeness (Mc) using the maximum curvature (MAXC) technique applied in the ZMAP Matlab code (Wiemer, 2001). This method worked quickly by defining the maximum curvature's point as the magnitude of completeness by computing the maximum value of the first derivative of the frequency-magnitude curve. The uncertainty was determined by a bootstrap approach. The comparison of FMD before and after performing MFT detection is provided in Fig. S3. The *b*- and *a*-values and their respective uncertainties are computed using a maximum-likelihood assessment (Shi and Bolt, 1982).

References:

Kennett, B. L. N., & Engdahl, E. R. (1991). Traveltimes for global earthquake location and phase identification. *Geophysical Journal International*, 105(2), 429-465.

Laske, G., Ma, Z., Masters, G., & Pasyanos, M. (2013). CRUST 1.0: A New Global Crustal Model at 1x1 degrees, http://igppweb.ucsd.edu/~gabi/crust1.html (accessed March 2020).

Lesage, P., Heap, M.J. & Kushnir, A. (2018). A generic model for the shallow velocity structure of volcanoes. *Journal of Volcanology and Geothermal Research*, 356, pp.114-126.

Shi, Y., & Bolt, B. A. (1982). The standard error of the magnitude-frequency b value. *Bulletin of the Seismological Society of America*, 72(5), 1677-1687.

Waldhauser, F., & Ellsworth, W. L. (2000). A double-difference earthquake location algorithm: Method and application to the northern Hayward fault, California. *Bulletin of the Seismological Society of America*, 90(6), 1353-1368.

Wiemer, S. (2001). A software package to analyze seismicity: ZMAP. *Seismological Research Letters*, 72(3), 373-382.

Figure S1. Similar plot with Fig. 2 for un-relocated epicenters.

Figure S2. Similar plot with Fig. 3 for un-relocated hypocenters.

Figure S3. Frequency-magnitude distribution (FMD) for (a) BMKG catalog or before MFT, and (b) MFT catalog.

Figure S4. Record of the 26 September 2017 M4.2 earthquake at station SRBI component vertical. (a) Raw data, (b) band-pass filtered 1-15 Hz, (c) spectrogram.

Figure S5. Similar plot with Fig. S4 for station DNP component vertical.

Figure S6. Record of the 8 November 2017 M4.9 earthquake at station SRBI component vertical. (a) Raw data, (b) band-pass filtered 1-15 Hz, (c) spectrogram.

Figure S7. Similar plot with Fig. S6 for station DNP component vertical.

Figure S8. Similar plot with Fig. 2, but the seismograms are for the 8 November 2017 M4.9.

Figure S9. Similar plot with Fig. 4 for the detection of 2017-09-21 09:07:17 M3.1 event. The black traces are for SNR<5 (not used in MFT).

Figure S10. Three-component seismograms at station SRBI for a newly detected event on 15 August 00:33:02.97 event.

Figure S11. Similar plot with Fig. S10 for 01:44:02.45 event.

Figure S12. Earthquake statistics using the MFT catalog. (a) Time histogram. (b) Depth histogram. (c) Magnitude histogram. (d) Cumulative seismic moment.

Table S1 List of relocated template candidates (templates library).

Table S2 Matched filter catalog.

> Mean CC= Mean correlation coefficient (Mean CC 1.0= self detection for 257 templates SNR>5).
>
> MAD= Median Absolute Deviation.

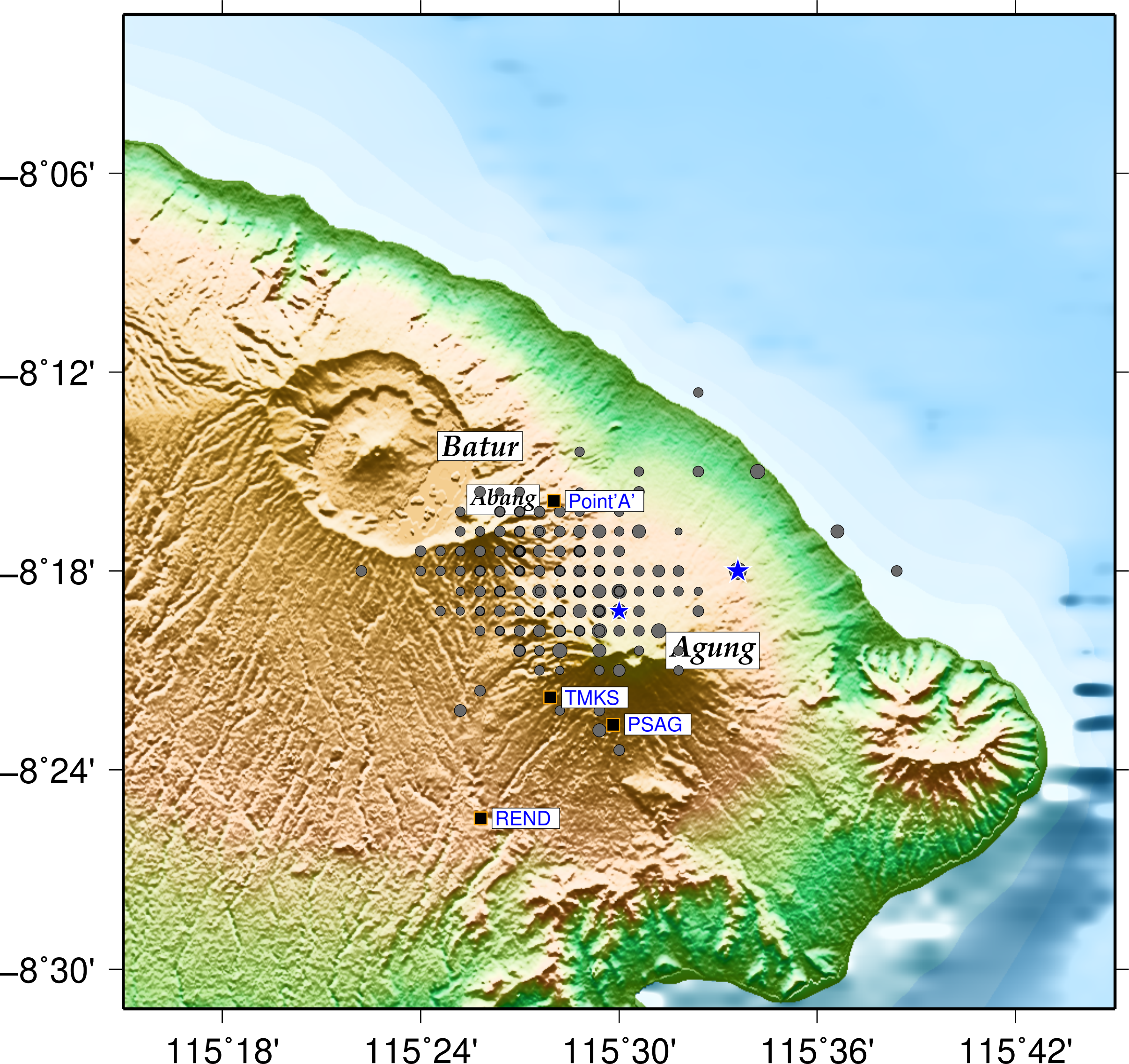

Batur
Abang
Point'A'
Agung
TMKS
PSAG
REND
−8˚06'
−8˚12'
−8˚18'
−8˚24'
−8˚30'
115˚18'
115˚24'
115˚30'
115˚36'
115˚42'

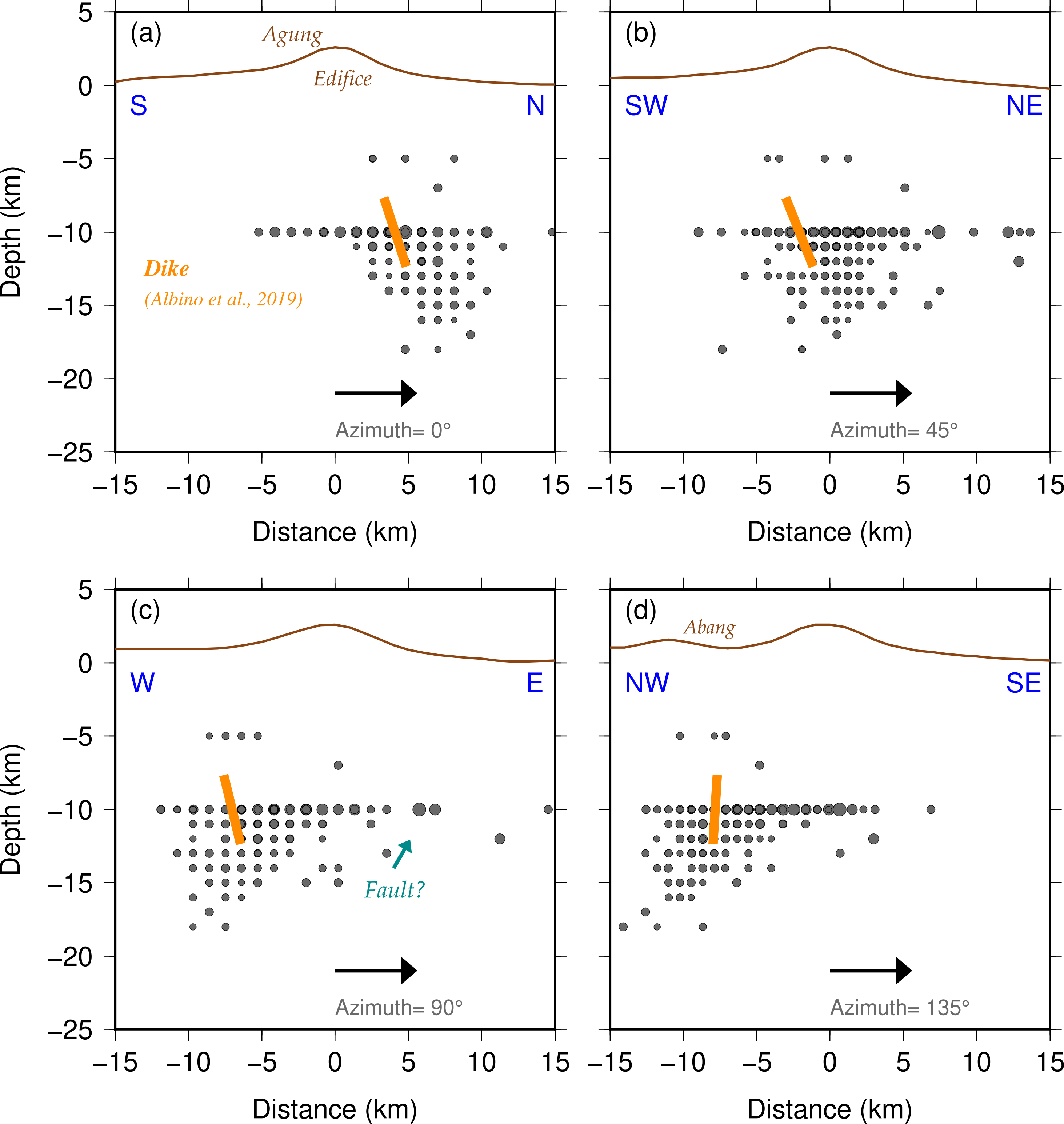

(a)
Agung
Edifice
S
N
Dike
(Albino et al., 2019)
Azimuth= 0°
(b)
SW
NE
Azimuth= 45°
(c)
W
E
Fault?
Azimuth= 90°
(d)
Abang
NW
SE
Azimuth= 135°
Depth (km)
Distance (km)
5
0
−5
−10
−15
−20
−25
−15
−10
−5
0
5
10
15

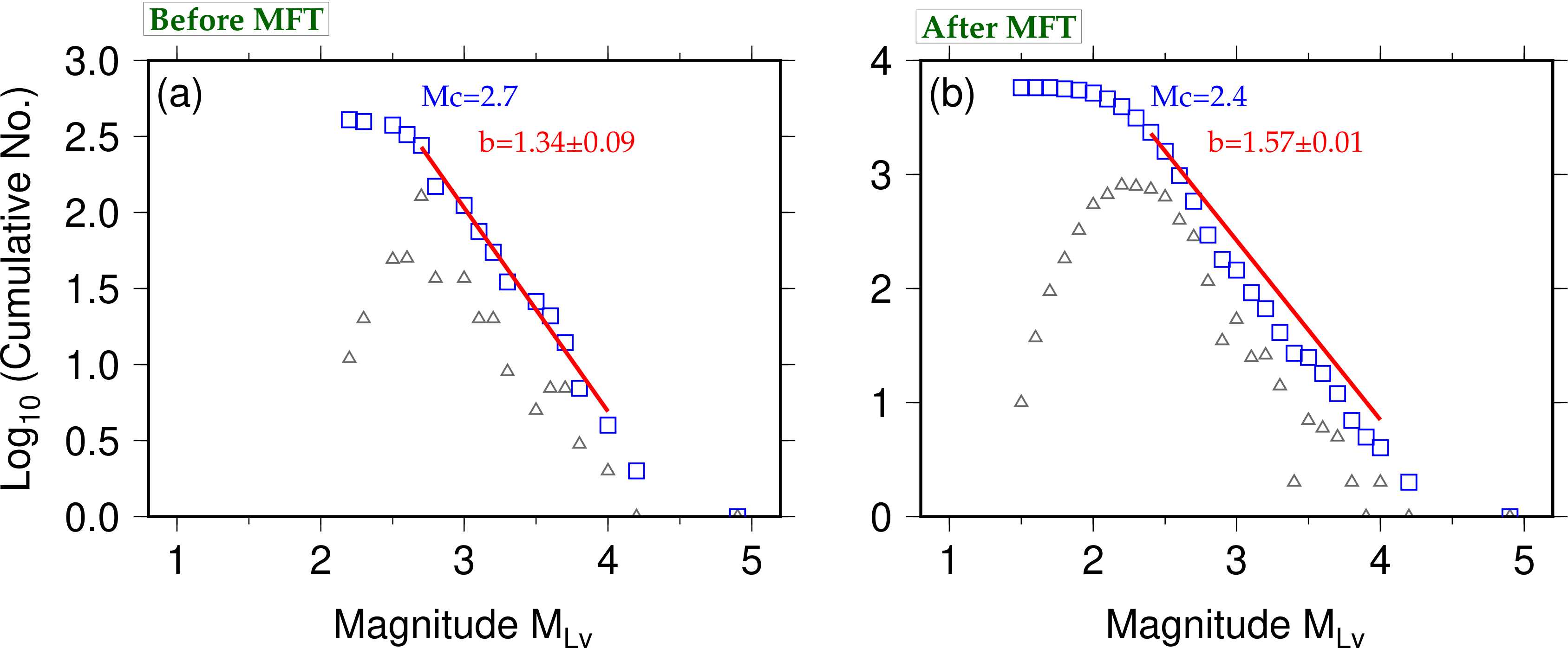

Before MFT
After MFT
(a)
(b)
Mc=2.7
b=1.34±0.09
Mc=2.4
b=1.57±0.01
Log10 (Cumulative No.)
Magnitude MLv
Magnitude MLv
0.0
0.5
1.0
1.5
2.0
2.5
3.0
0
1
2
3
4
1
2
3
4
5
1
2
3
4
5

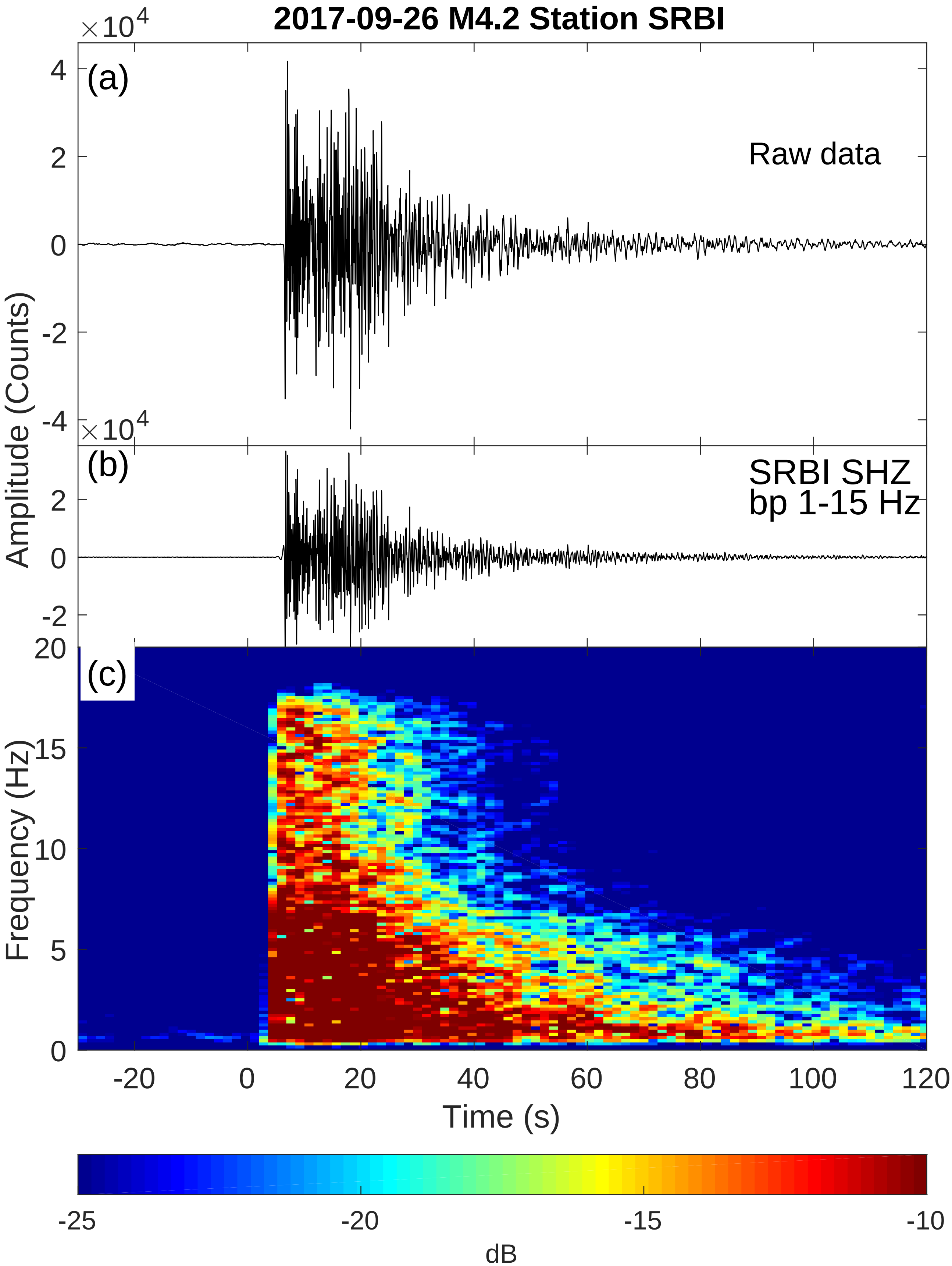
2017-09-26 M4.2 Station SRBI
(a)
Raw data
(b)
SRBI SHZ
bp 1-15 Hz
(c)
Amplitude (Counts)
Frequency (Hz)
Time (s)
dB

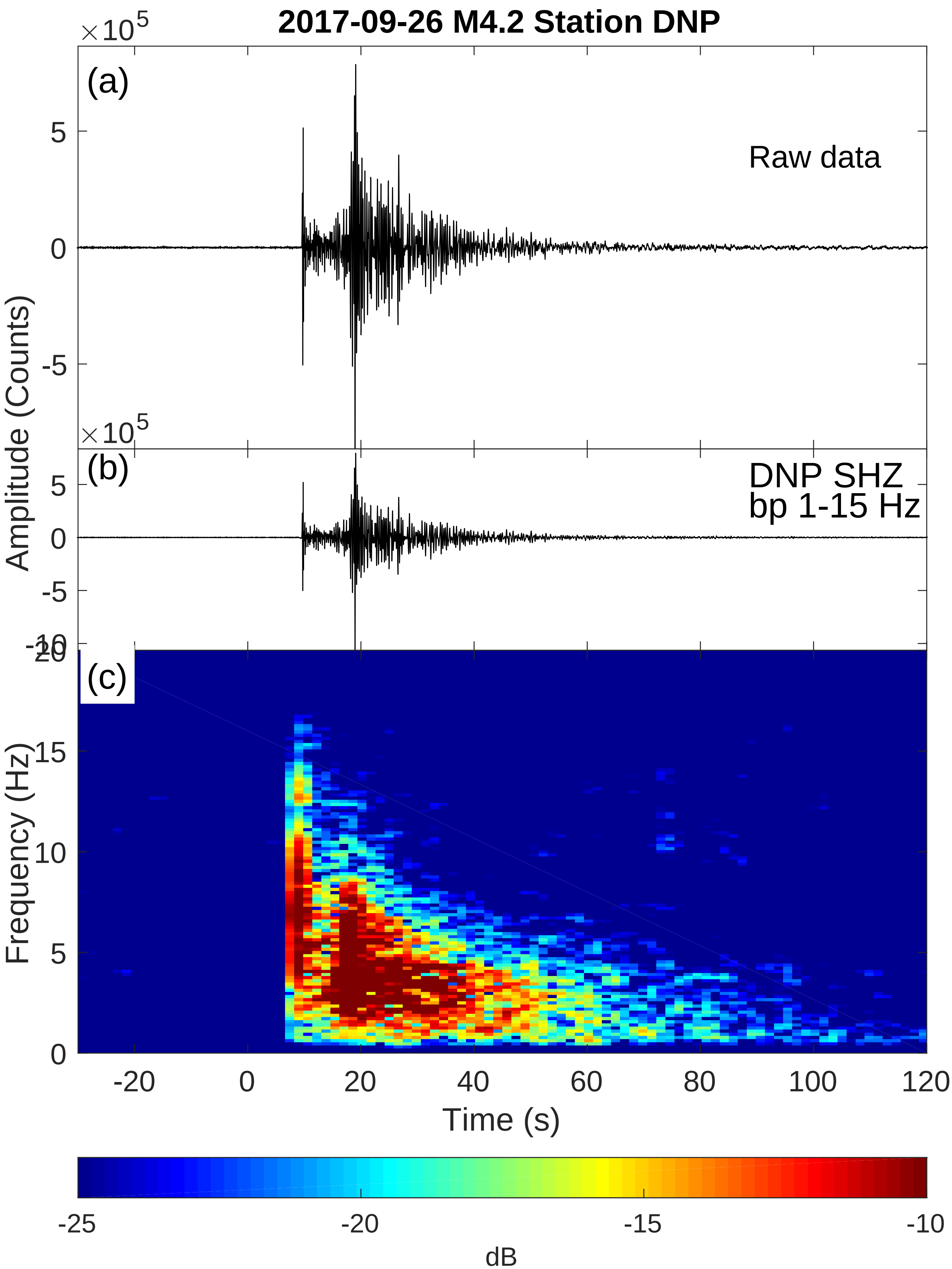

2017-09-26 M4.2 Station DNP
(a)
Raw data
(b)
DNP SHZ
bp 1-15 Hz
(c)
Amplitude (Counts)
Frequency (Hz)
Time (s)
dB

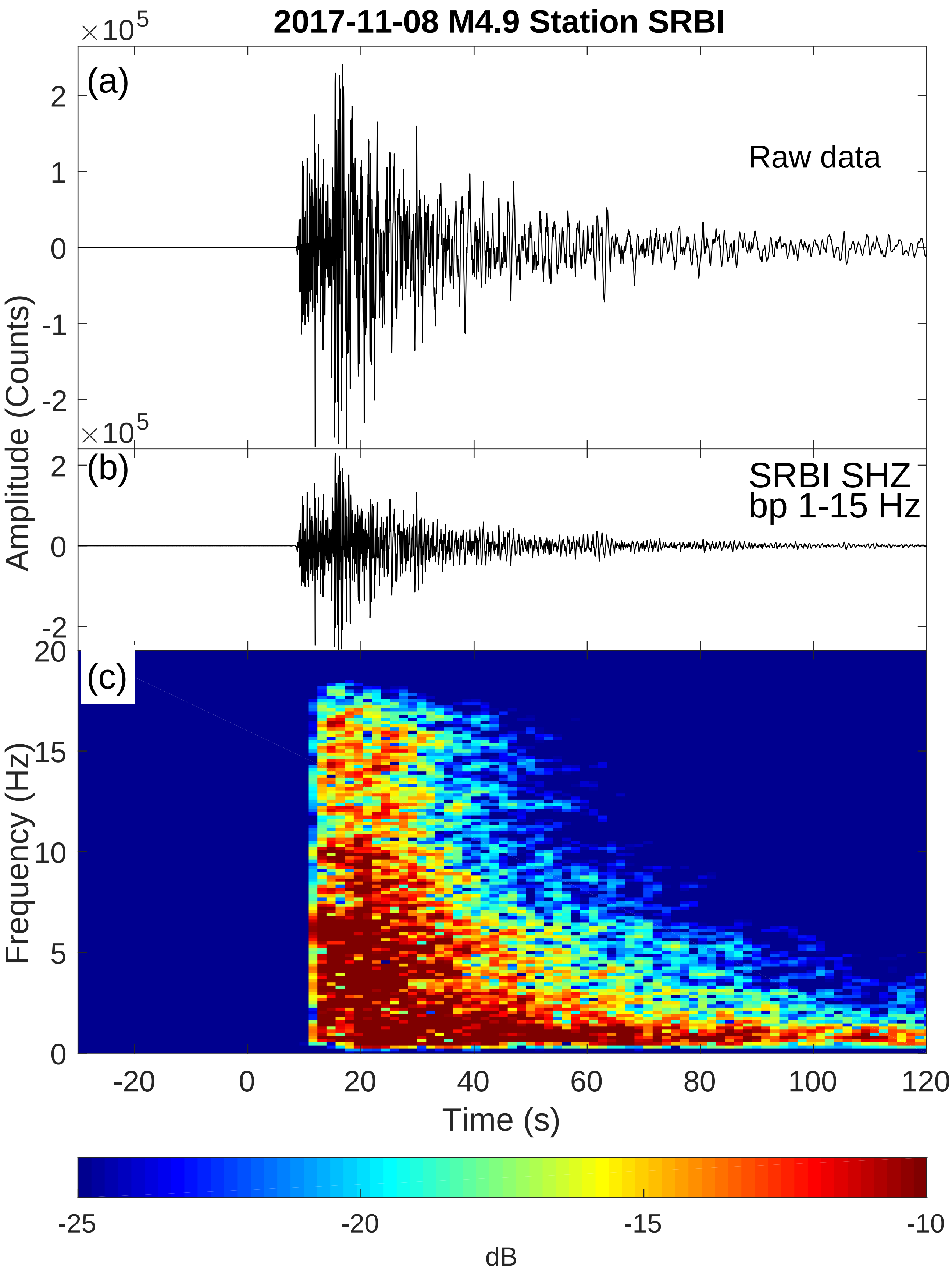
2017-11-08 M4.9 Station SRBI
(a)
Raw data
(b)
SRBI SHZ
bp 1-15 Hz
(c)
Amplitude (Counts)
Frequency (Hz)
Time (s)
dB

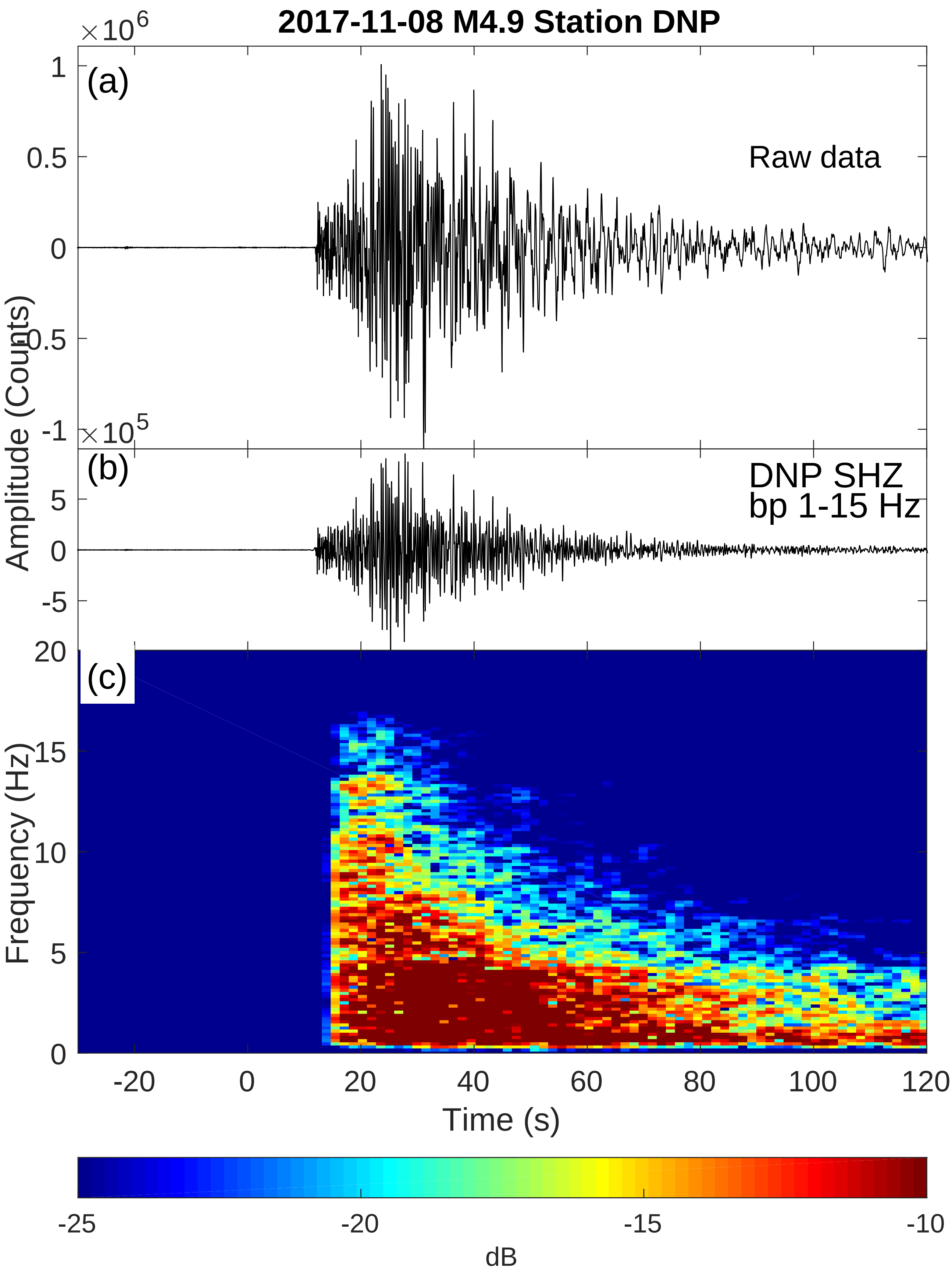

2017-11-08 M4.9 Station DNP
(a)
Raw data
(b)
DNP SHZ
bp 1-15 Hz
(c)
Amplitude (Counts)
Frequency (Hz)
Time (s)
dB

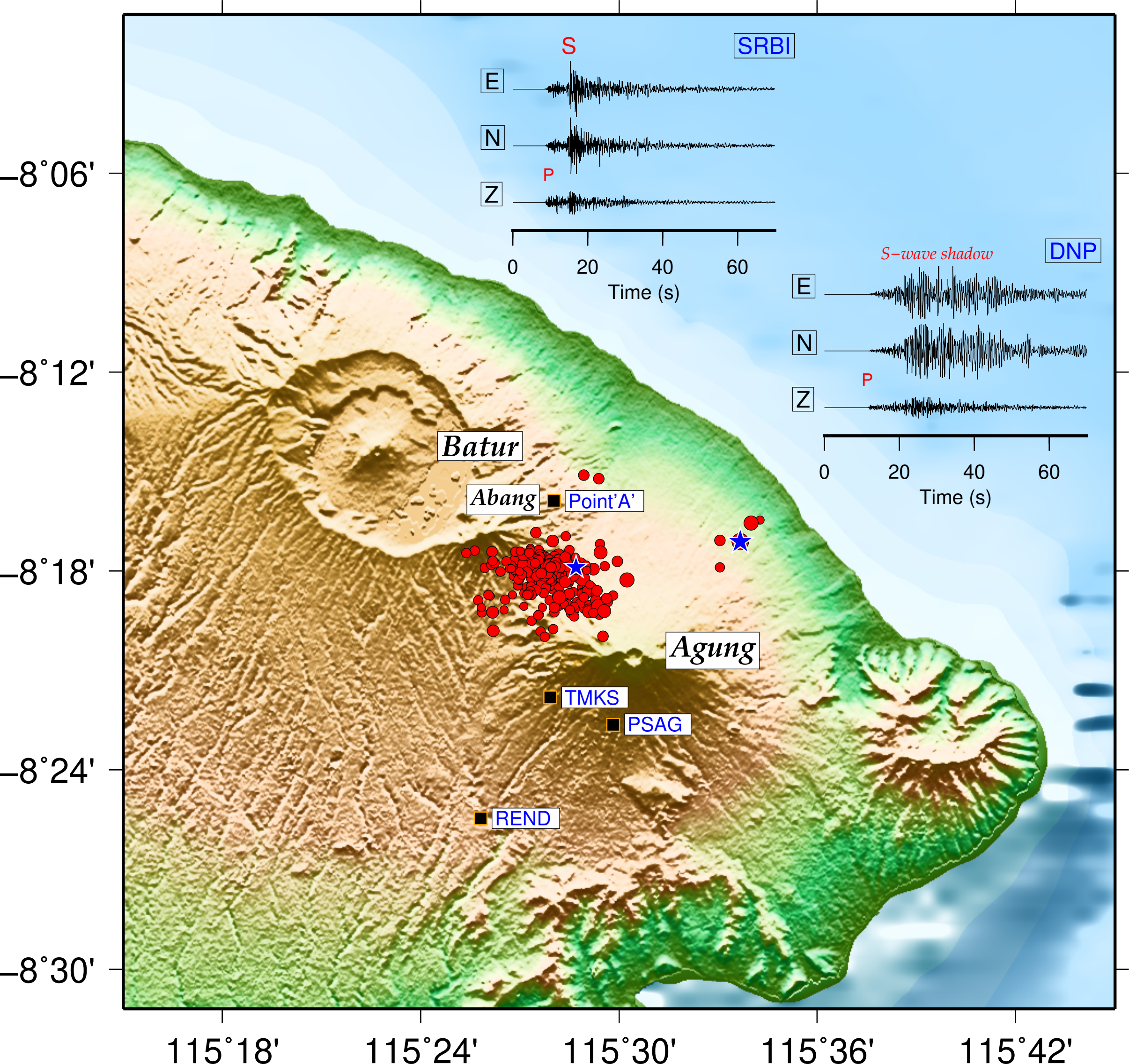

S
SRBI
E
N
P
Z
0
20
40
60
Time (s)
S−wave shadow
DNP
E
N
P
Z
0
20
40
60
Time (s)
Batur
Abang
Point'A'
Agung
TMKS
PSAG
REND
−8˚06'
−8˚12'
−8˚18'
−8˚24'
−8˚30'
115˚18'
115˚24'
115˚30'
115˚36'
115˚42'

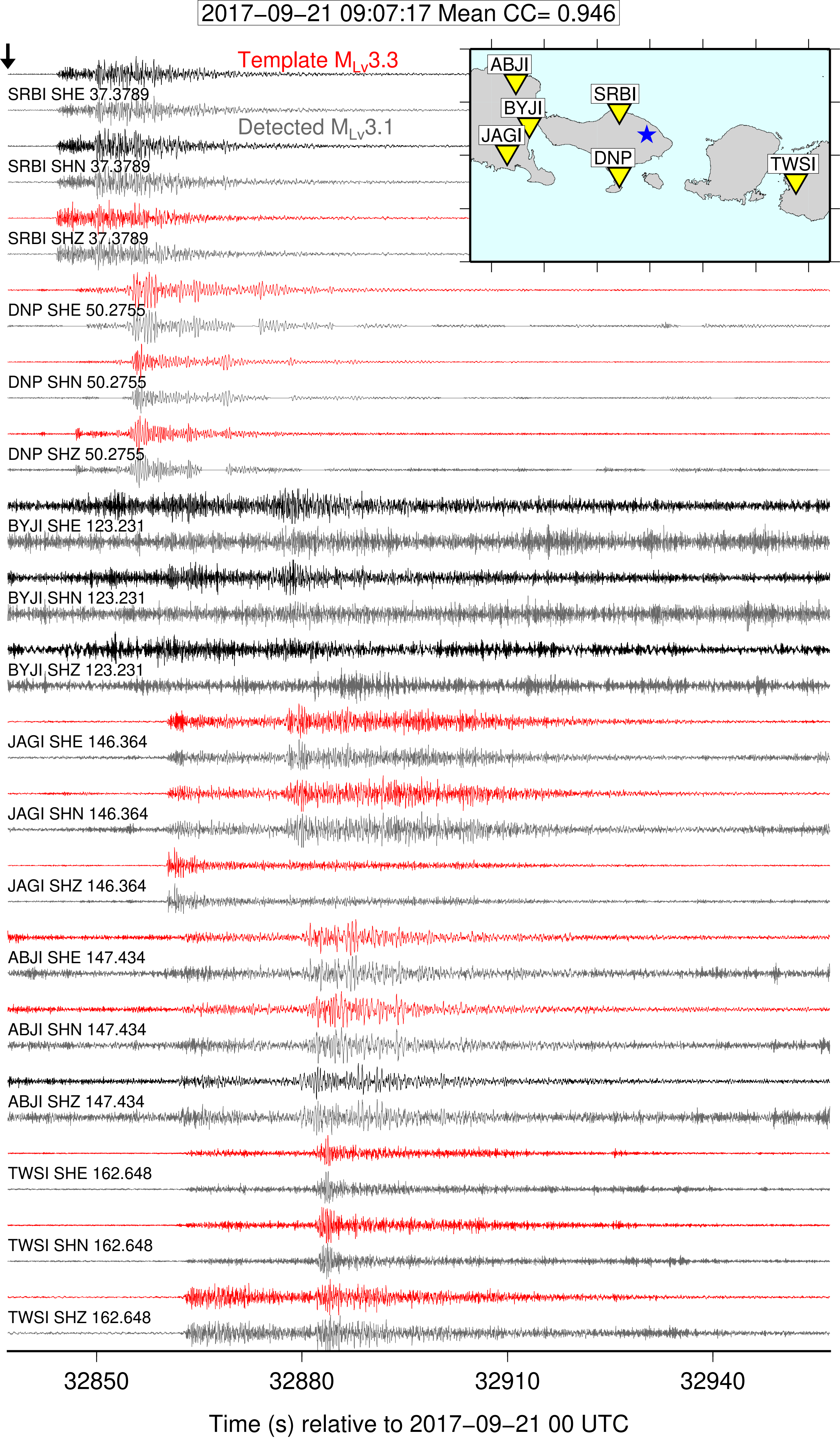
2017−09−21 09:07:17 Mean CC= 0.946
Template M_{Lv}3.3
Detected M_{Lv}3.1
SRBI SHE 37.3789
SRBI SHN 37.3789
SRBI SHZ 37.3789
DNP SHE 50.2755
DNP SHN 50.2755
DNP SHZ 50.2755
BYJI SHE 123.231
BYJI SHN 123.231
BYJI SHZ 123.231
JAGI SHE 146.364
JAGI SHN 146.364
JAGI SHZ 146.364
ABJI SHE 147.434
ABJI SHN 147.434
ABJI SHZ 147.434
TWSI SHE 162.648
TWSI SHN 162.648
TWSI SHZ 162.648
ABJI
BYJI
JAGI
SRBI
DNP
TWSI
32850
32880
32910
32940
Time (s) relative to 2017−09−21 00 UTC

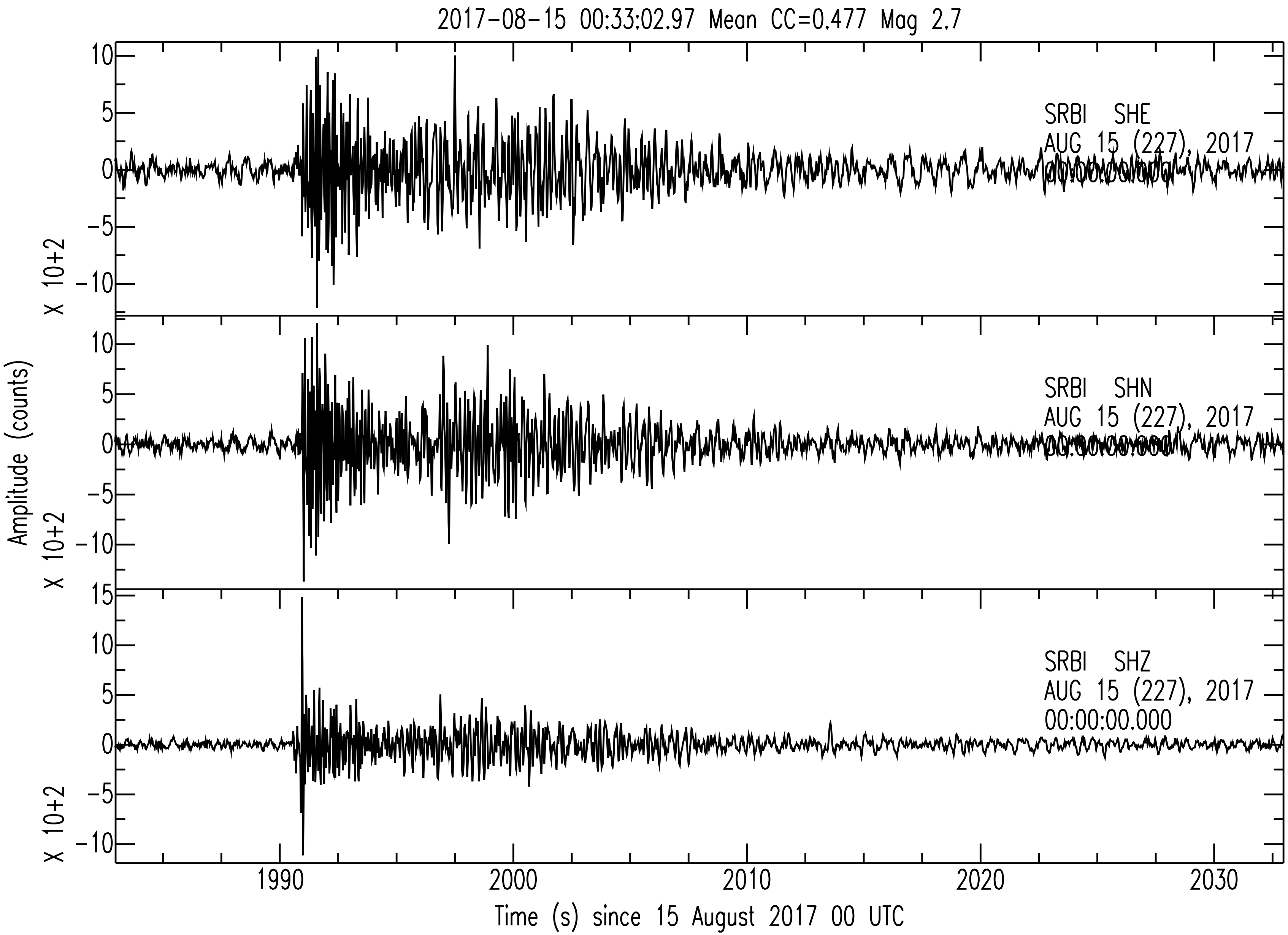
2017-08-15 00:33:02.97 Mean CC=0.477 Mag 2.7
SRBI SHE
AUG 15 (227), 2017
SRBI SHN
AUG 15 (227), 2017
SRBI SHZ
AUG 15 (227), 2017
00:00:00.000
Amplitude (counts)
X 10+2
Time (s) since 15 August 2017 00 UTC

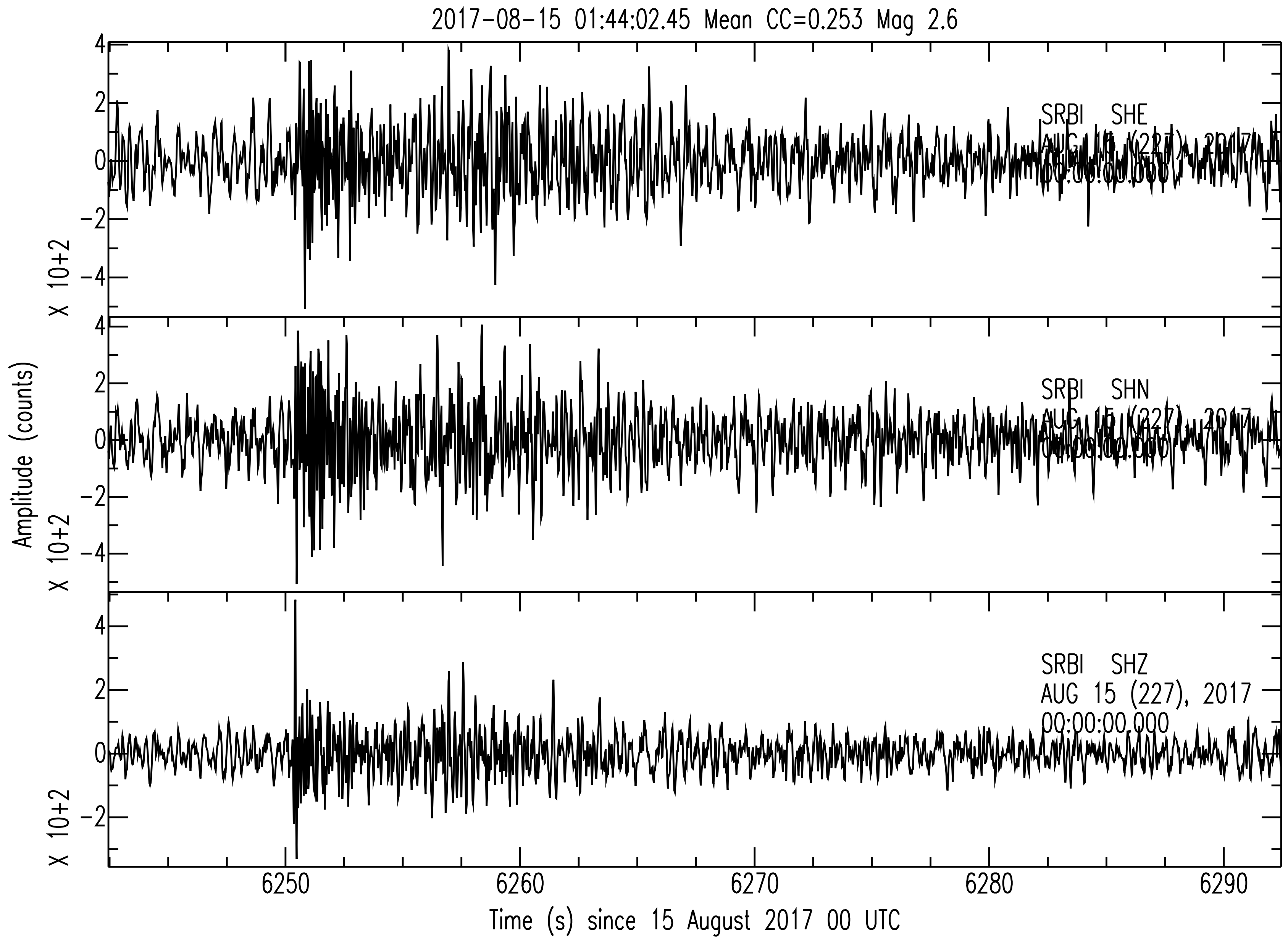
2017-08-15 01:44:02.45 Mean CC=0.253 Mag 2.6
SRBI SHE
SRBI SHN
SRBI SHZ
AUG 15 (227), 2017
00:00:00.000
Amplitude (counts)
X 10+2
4
2
0
-2
-4
6250
6260
6270
6280
6290
Time (s) since 15 August 2017 00 UTC

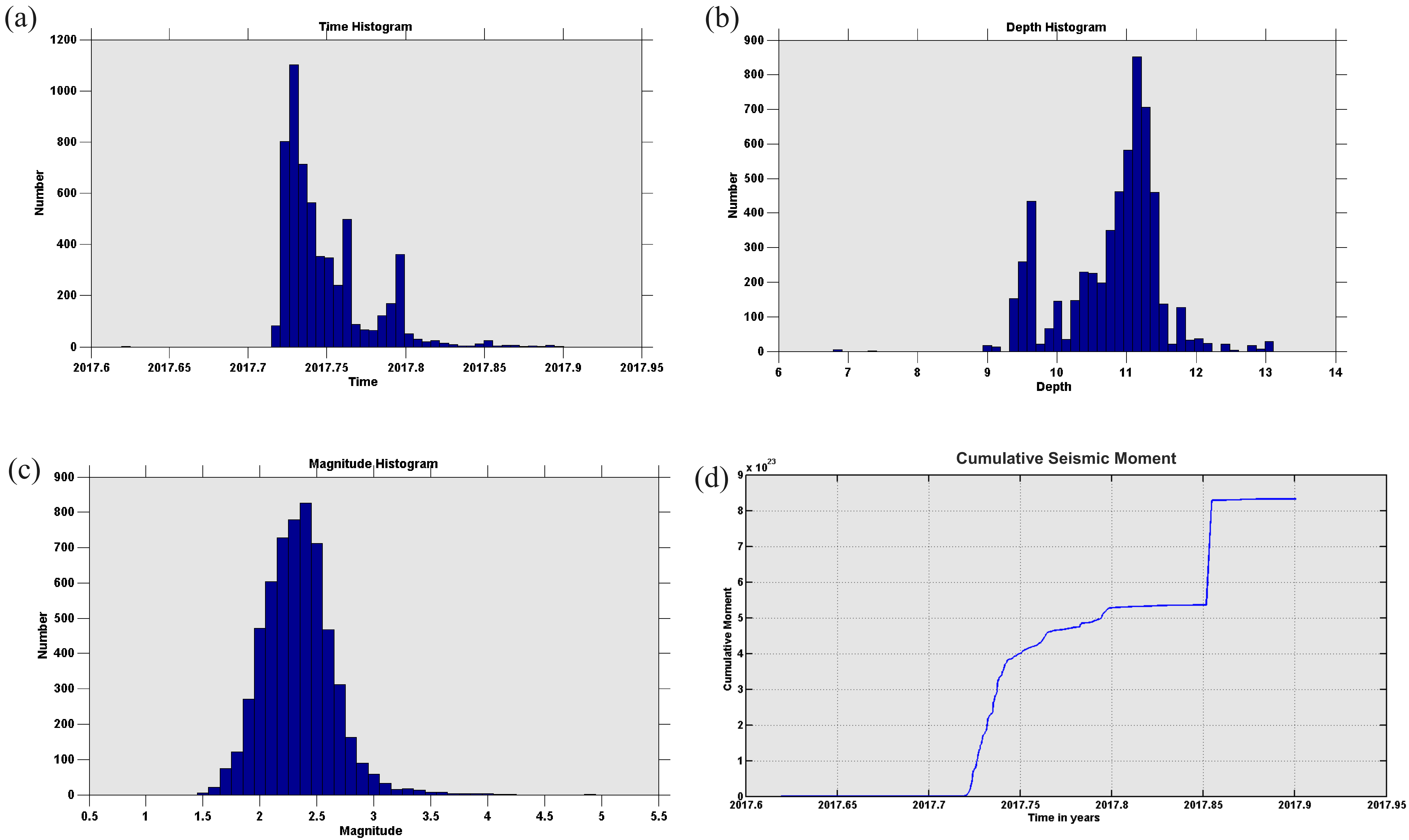

(a)
Time Histogram
Number
Time
(b)
Depth Histogram
Number
Depth
(c)
Magnitude Histogram
Number
Magnitude
(d)
Cumulative Seismic Moment
x 10^23
Cumulative Moment
Time in years